Cell Reports

Article

Critical role of WASp in germinal center tolerance through regulation of B cell apoptosis and diversification

Graphical abstract

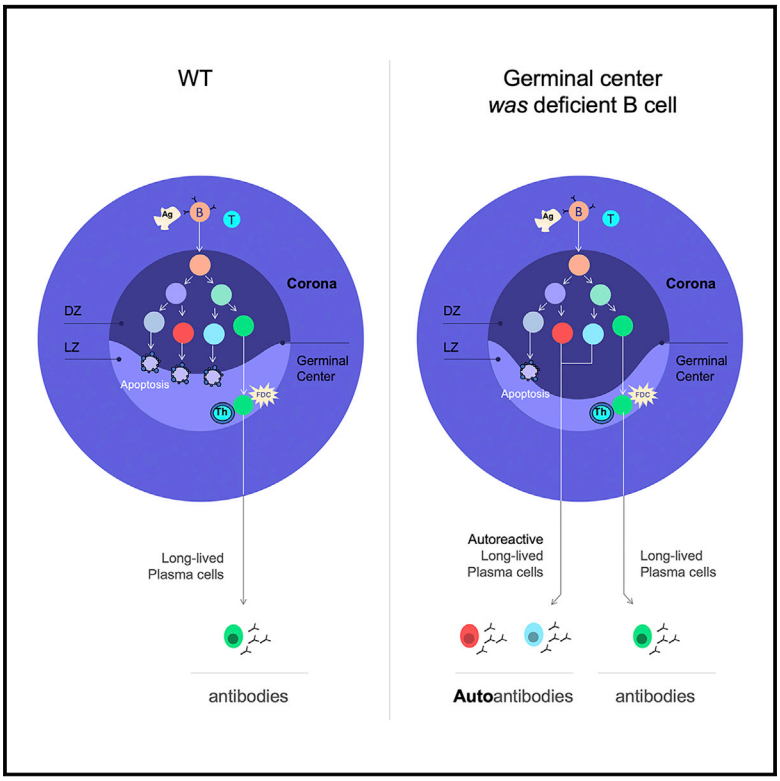

Authors

Marc Descatoire, Remi Fritzen, Samuel Rotman, ..., Adrian J. Thrasher, Elisabetta Traggiai, Fabio Candotti

Correspondence

marc.descatoire@chuv.ch

In brief

Descatoire et al. show that deletion of Wiskott-Aldrich syndrome (WAS) protein from germinal center B cells leads to reduced B cell apoptosis and broad autoimmunity that is dependent on B cell diversification, pointing to a critical role of WASp in the tolerance mechanisms at play in the germinal center reaction.

Highlights

- WASp is highly expressed in germinal center B cells, suggesting its relevance *in situ*
- WASp-defective mouse germinal center B cells are sufficient to induce autoimmunity
- WASp-defective germinal center B cells show lower apoptosis rate
- WASp-defective B cells acquire self-reactivity during the germinal center reaction

Descatoire et al., 2022, Cell Reports *38*, 110474
March 8, 2022
https://doi.org/10.1016/j.celrep.2022.110474

CellPress

Cell Reports

CellPress
OPEN ACCESS

Article

Critical role of WASp in germinal center tolerance through regulation of B cell apoptosis and diversification

Marc Descatoire,[1,6,*] Remi Fritzen,[2] Samuel Rotman,[3] Genevieve Kuntzelman,[4] Xavier Charles Leber,[4] Stephanie Droz-Georget,[1] Adrian J. Thrasher,[5] Elisabetta Traggiai,[4] and Fabio Candotti[1]

[1]Laboratory of Inherited Immune Disorders, Division of Immunology and Allergy, Lausanne University Hospital and University of Lausanne, Lausanne, Switzerland
[2]University of St Andrews, St Andrews, UK
[3]Service of Clinical Pathology, Lausanne University Hospital and University of Lausanne, Lausanne, Switzerland
[4]Novartis Institutes for BioMedical Research, Basel, Switzerland
[5]University College of London, Great Ormond Street Institute of Child Health, London, UK
[6]Lead contact
*Correspondence: marc.descatoire@chuv.ch
https://doi.org/10.1016/j.celrep.2022.110474

SUMMARY

A main feature of Wiskott-Aldrich syndrome (WAS) is increased susceptibility to autoimmunity. A key contribution of B cells to development of these complications has been demonstrated through studies of samples from affected individuals and mouse models of the disease, but the role of the WAS protein (WASp) in controlling peripheral tolerance has not been specifically explored. Here we show that B cell responses remain T cell dependent in constitutive WASp-deficient mice, whereas selective WASp deletion in germinal center B cells (GCBs) is sufficient to induce broad development of self-reactive antibodies and kidney pathology, pointing to loss of germinal center tolerance as a primary cause leading to autoimmunity. Mechanistically, we show that WASp is upregulated in GCBs and regulates apoptosis and plasma cell differentiation in the germinal center and that the somatic hypermutation-derived diversification is the basis of autoantibody development.

INTRODUCTION

In the bone marrow (BM), receptor editing and clonal deletion prevent immature B cells expressing B cell receptors (BCR) reactive to local and systemic self-antigens from continuing development and constitute the central tolerance checkpoint (Nemazee, 2017). The reduced breadth of antigens against which developing B cells in the BM are tested leads to survival and release in the periphery of high proportions (≈20%) of mature, self-reactive, naive B cells (Wardemann et al., 2003). Lack of cognate T cell helper interaction and/or suppression by $FOXP3^+$ $CD4^+$ regulatory T (Treg) cells prevents activation of these self-reactive naive B cells in the periphery. This process, known as the "two-signal model" (Bretscher and Cohn, 1970), together with cell-intrinsic mechanisms induced by exposure of B cells to autoantigens leading to functional non-responsiveness (anergy) limits the frequency of autoreactive naive B cells that can enter the germinal center reaction (Cambier et al., 2007) and constitutes an important peripheral B cell tolerance checkpoint.

Central to protective humoral immune responses is the role of germinal centers (GCs) in production of high-affinity, long-lived plasma cells and memory B cells. Affinity maturation of GC B cells (GCBs) occurs through random acquisition of somatic hypermutations (SHMs) in their BCRs. The activation-induced cytidine deaminase (AID) enzyme regulates this process (Muramatsu et al., 2000; Revy et al., 2000). Independent of its mutational activity, AID is also essential for immunoglobulin class switch recombination (CSR) (Shinkura et al., 2004; Wei et al., 2011). SHM can result in emergence of self-reactivity (Tiller et al., 2007), which is controlled by an additional peripheral tolerance checkpoint that avoids selection of self-reactive cells. Deletion of GCBs interacting *in situ* with self-antigens (Chan et al., 2012) or redemption by continuous mutation followed by selection (Burnett et al., 2018) leads to removal of some self-reactive GCBs. According to current models of the GC reaction, apoptosis of cells that have lost specificity for the antigen (and therefore may have acquired self-reactivity) is also an important contributor to peripheral maintenance of tolerance. Inhibition of apoptosis leads to autoimmunity with development of autoantibodies. Finally, selection of B cells with high-affinity BCRs requires alternating migration of GCBs from the dark zone (DZ) to the light zone (LZ) of the GC, regulated by a series of actin-dependent cellular processes (e.g., chemotaxis, BCR endocytosis, immune synapse formation, major histocompatibility complex [MHC] class II recycling), whose importance is highlighted by the increasing number of actin-related gene deficiencies that have been reported to be associated with defective GCB selection (He and Westerberg, 2019).

Among such disorders is Wiskott-Aldrich syndrome (WAS), a rare X-linked disease presenting with thrombocytopenia and variable susceptibility to eczema, recurrent infections, autoimmunity, and cancer (Candotti, 2018). WAS is caused by genetic deficiency of the WAS protein (WASp), the founding member of a family of actin nucleation-promoting factors that translate surface signals into actin polymerization through the actin-related protein Arp2/3 complex (Kelly et al., 2006). Biological defects have been described in most hematological lineages from individuals with WAS, which is consistent with the pattern of expression of WASp across the hematopoietic system and the wide breadth of clinical features of the disease (Bosticardo et al., 2009). A prominent clinical feature of WAS is increased susceptibility to autoimmunity, with 40%–71% of affected individuals developing at least one autoimmune complication, which suggests a pivotal role of WASp in maintenance of central and/or peripheral tolerance to self-antigens.

The specific B cell contribution to autoimmunity in WAS has been studied with early conditional knockout mouse models (B/WcKO), in which *Was* is deleted in BM precursor B cells (Recher et al., 2012), or in WASp-deficient B cell chimera models (WBchim) (Becker-Herman et al., 2011). These experiments have shown that intrinsic defects of WASp-deficient B cells result in development of autoantibodies and autoimmunity that correlate with a higher frequency of development of spontaneous GCs (sptGCs) (Recher et al., 2012; Becker-Herman et al., 2011). Mechanisms of central B cell tolerance have been reported to be functional in WASp-deficient mice (Kolhatkar et al., 2015), but the role of WASp in maintenance of peripheral B cell tolerance has not been completely dissected.

We generated a ROSA26-YFP reporter mouse model in which the *Was* gene is floxed and deleted in GCBs by expressing the Cre recombinase under control of the constant gamma 1 heavy-chain promotor (Cγ1cre) (Casola et al., 2006). Analysis of these mice (GCBWcKO) showed reduced apoptosis in WASp-deficient GCBs and increased plasma cell differentiation. Importantly, WASp deficiency in GCBs was sufficient to yield broad development of autoantibodies and immune complex-mediated kidney disease despite the naive B cell compartment being unaffected and in the absence of increased sptGC development. In addition, we demonstrate that GCB diversification is required for development of immunoglobulin G (IgG) anti-DNA autoantibodies. Finally, we took advantage of the immunological ignorance of C57BL/6 mice for the hen egg lysozyme (HEL) antigen (Chaouat et al., 1991) to demonstrate that T cell-dependent control of peripheral B cell responses is functional in constitutive WASp-deficient (*Was* KO) mice and that antibody responses to HEL are strongly reduced in this model in the absence of GCB diversification. Our results point to defects of GC mechanisms enforcing tolerance as the cause leading to autoimmunity in WASp deficiency.

RESULTS

GCBs express high levels of WASp

To begin exploring the role of WASp in the GC, we assessed expression of WASp in $Cy1^{cre/WT}$ ROSA26-YFP reporter control (CTL) mice immunized intraperitoneally with human red blood cells (hRBCs). Late plasmablasts (PBs)/plasma cells (PCs) were identified by their YFP^+ $CD19^{low/-}$ $CD138^{high}$ profile. Among $CD19^+$ cells, classic GCBs and early-differentiated PB/PCs ($CD138^{high}$) can be identified among $CD95^+$ IgD^- cells, whereas the $CD95^-$ fraction contains IgM^{low} IgD^{high} follicular (FO) B cells and IgM^{high} IgD^{high} immature transitional B lymphocytes (Figures 1A and 1B). The levels of WASp expression in the various B cell subsets were heterogeneous. To account for cell size differences in activated versus resting and differentiated versus non-differentiated cells, we assessed the ratio between WASp mean fluorescence intensity (MFI) and cell size. This analysis identified GCBs as the B cell mature subset with the highest expression of WASp and revealed a marked reduction of WASp expression in differentiated PBs/PCs (Figure 1C). These findings suggested that WASp is important for GCB function(s) and prompted us to develop a mouse model of WASp deficiency in GCBs by crossing *Was* gene-floxed mice (Recher et al., 2012) with the Cγ1cre ROSA26-YFP model, which expresses the Cre recombinase under control of Cγ1cre promoter (Casola et al., 2006). As expected, YFP^+ GCBs and post-GCBs (PBs/PCs) from the resulting animals (GCBWcKO) did not express WASp, whereas transitional and FO B cells retained normal WASp expression levels, as did most YFP^- GCBs (Figure 1D). Thus, in the GCBWcKO model, YFP expression correlates with *Was* gene deletion.

As anticipated based on the Cy1cre ROSA26-YFP model (Casola et al., 2006), Cre recombination occurred efficiently in GCBs from CTL and GCBWcKO hRBC-immunized animals, as assessed by YFP expression (91.4% ± 3% of CTL GCBs and 84.6% ± 6.6% of GCBWcKO GCBs), whereas only minor fractions of naive IgD^+ B cells appeared YFP^+ in both strains (3.36% ± 0.58% versus 1.80% ± 0.62%) (Figure 2A). Surprisingly, frequencies of recombined cells (YFP^+) were markedly reduced in GCBs from unimmunized mice because of a high frequency of IgM^+ cells (Figure S1), but no differences were noted between CTL and GCBWcKO animals (38.9% ± 8.10% versus 38.7% ± 7.87%), whereas the IgD^+ B cell compartment remained almost completely YFP negative (Figure 2B).

Was deletion in GCBs is sufficient to induce autoimmunity in the absence of increased sptGCs

A consistent feature of WASp-deficient mouse models is development of autoantibodies and autoimmune complications (Becker-Herman et al., 2011; Recher et al., 2012). Therefore, we analyzed sera from 6-month-old unimmunized GCBWcKO mice and demonstrated significant levels of IgG anti-double-stranded DNA (dsDNA) and anti-single-stranded DNA (ssDNA) autoantibodies (Figure 3A). Sera from 1-year-old CTL and GCBWcKO unimmunized mice were also assessed by protein chip assay on 13,788 targets. GCBWcKO mice showed significantly increased levels of autoantibodies for a large number of autoantigens (210 with $p \leq 0.005$, 42 with $p \leq 0.001$, and 7 with $p \leq 0.0001$) (Figures 3B and 3C; Table S1). Interestingly, among the most significant targets for the detected autoantibodies were interleukin-4 (IL-4) and IL-6, critical cytokines produced during the GC reaction. Anti-DNA autoantibodies were also detected, which confirms and validates DNA as an early, relevant self-antigen for assessment of breach in B cell tolerance

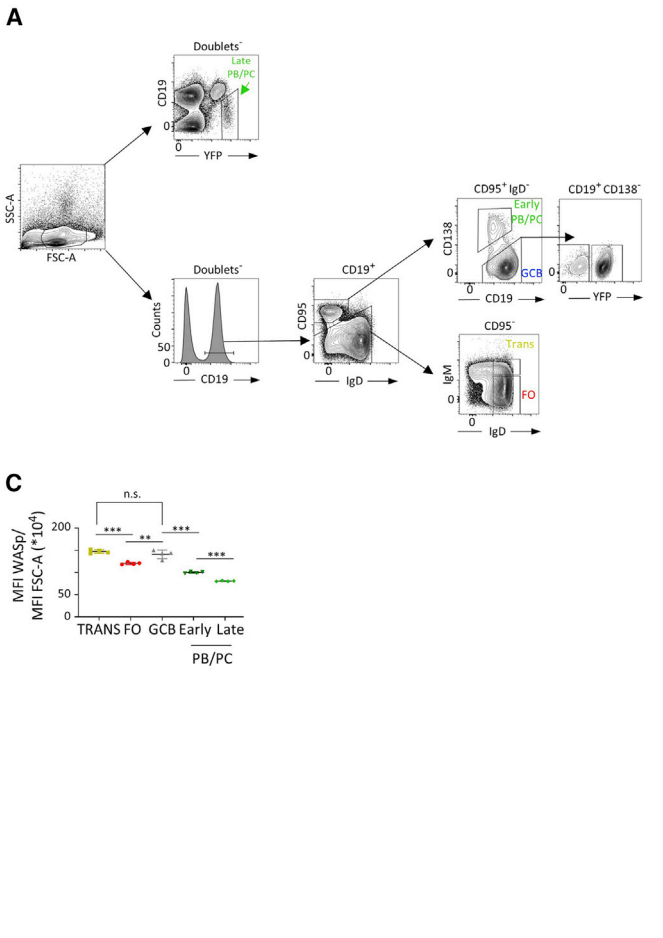

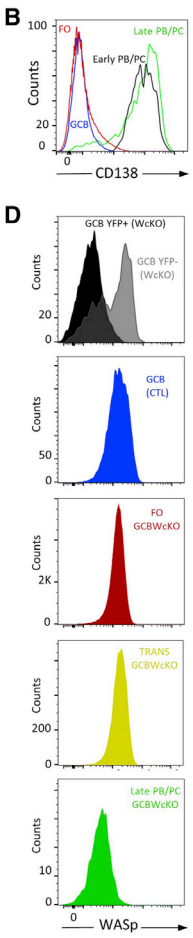

Figure 1. GCBs express high levels of WASp

(A) Gating strategy for follicular (FO), transitional (Trans), and YFP$^+$ and YFP$^-$ GC B cells (GCB) and early and late plasmablasts (PBs)/plasma cells (PCs).

(B) Representative histogram plots showing the CD138 staining profile of FO (red line), late PCs (green line), early PCs (black line), and GCBs (blue line) from CTL mice.

(C) Mean fluorescent Intensity (MFI) of WASp relative to cell size (mean ± SD). Data are representative of 3 different experiments.

(D) Representative WASp expression levels in YFP$^+$ (solid black) and YFP$^-$ (solid gray) GCBs, FO (red), Trans (orange), and PCs (green) from GCBWcKO mice. WASp expression in GCBs from CTL mice (blue) is shown for reference.

Statistical significance is indicated on graphs as determined by unpaired Student's t test. **p < 0.01, ***p < 0.001.

in models of WASp deficiency (Arkatkar et al., 2017; Dahlberg et al., 2015; Jackson et al., 2016; Recher et al., 2012; Humblet-Baron et al., 2007; Becker-Herman et al., 2011). We also observed that GCBWcKO mice showed IgG kidney deposits in the form of subendothelial and mesangial immune complexes, revealed by electronic microscopy, that correlated with signs of glomerular hypercellularity (Figure 3D), suggesting pathogenic consequences of the immune dysregulation features of GCBWcKO mice.

Development of anti-DNA antibodies in *Was* KO, B/WcKO, and WBchim mice (Recher et al., 2012; Becker-Herman et al., 2011; Arkatkar et al., 2017; Jackson et al., 2016) and IgG kidney deposits (Becker-Herman et al., 2011) have been associated with an increased frequency of sptGCs. It was significant, therefore, that 6-month-old unimmunized GCBWcKO mice did not show an increased frequency of sptGCs (0.99% ± 0.62% versus 1.03% ± 0.72%). On the other hand, immunized GCBWcKO mice showed a slight but significant reduction in GCB frequency compared with CTL mice (2.85% ± 1.29% versus 4.06% ± 0.61%, $p \leq 0.01$), which is consistent with the known delayed GC reaction development in WASp deficiency (Westerberg et al., 2005; Figure 3E). These findings indicate that *Was* deletion in GCBs is sufficient to induce autoimmunity in the absence of increased sptGC development. These observations also strongly suggest that the generation of sptGCs observed in models in which WASp expression is deleted in B cell precursors (Becker-Herman et al., 2011; Recher et al., 2012) is due to spontaneous activation of WASp-deficient, naive B cells.

WASp-deficient PCs are less diversified

A possible mechanism for generation of autoantibodies is biased selection of self-reactive GCBs that differentiate into PCs. To assess whether WASp deficiency in GBCs resulted in biased selection of WASp-deficient BM PCs, we sorted B220$^-$ IgD$^-$ CD138$^+$ PCs from BM cells of CTL and GCBWcKO mice. From the latter, we separated YFP$^-$ (*Was*$^+$) and YFP$^+$ (*Was*-deleted) cells. We then sequenced the J_H4 intronic region of the Ig heavy-chain locus to assess the frequency of mutated sequences and somatic mutations. As shown in Figure 4A, almost 100% of sequences from CTL mice were mutated. For 2 of 3 GCBWcKO mice, sequences from *Was*-retaining, YFP$^-$ cells were 100% mutated, with 89% mutated sequences observed in cells from the third animal. A higher proportion of germline sequences was found in their *Was*-deleted, YFP$^+$ counterparts, with 67%, 83%, and 89% of sequences mutated. Moreover, the mutation frequency was significantly reduced among mutated clones from YFP$^+$ cells (0.75% ± 0.25%) compared with their YFP$^-$ counterparts (1.82% ± 0.2%) and CTL pPCs (1.91% ± 0.64%) (Figure 4B), with an average frequency of mutations per individual sequence that was 2.4 times less among YFP$^+$ clones than in YFP$^-$ cells (3.33% ± 1.08% versus 8.08% ± 0.86%, $p \leq 0.05$) (Figure 4C). Thus, selection of *Was*-deleted PCs appears to be strongly biased toward germline and poorly mutated cells. Consistent with an altered SHM process, we observed that GCBWcKO mice showed significantly lower affinity maturation of antibodies when

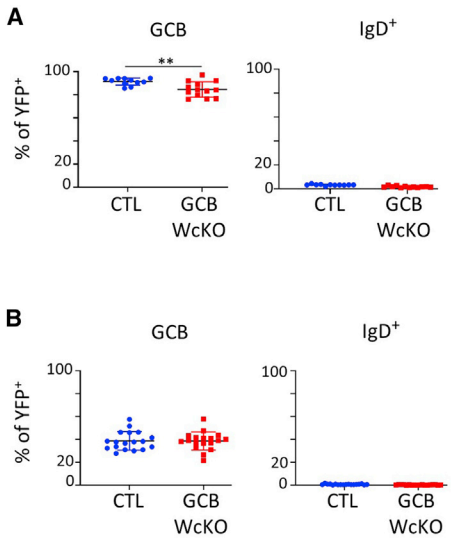

Figure 2. Characterization of GCB development and Cre recombination efficiency in unimmunized and immunized mice

(A) Frequencies of YFP$^+$ (*Was*-deleted) cells among GCBs and IgD$^+$ B cells from hRBC-immunized CTL and GCBWcKO mice analyzed at 14 d.p.i.

(B) Frequencies of YFP$^+$ (*Was*-deleted) cells among sptGCBs and IgD$^+$ B cells from unimmunized CTL and GCBWcKO mice.

Data are from three independent experiments (mean ± SD). IgD$^+$ B cells were gated as living CD19$^+$ GL7$^-$ and GCB as living CD19$^+$ GL7$^+$ IgD$^-$. Statistical significance is indicated on graphs as determined by unpaired Student's t test. **$p < 0.01$.

immunized with 4-hydroxy-3-nitrophenyl) acetyl-conjugated bovine serum albumin (NP-BSA) (Figure S2).

To test whether poorly mutated PCs are responsible for development of autoantibodies, we used AIDG23S mutant mice, in which SHM is strongly impaired but CSR is preserved (Wei et al., 2011), to generate the AID$^{G23S/G23S}$ Cγ1$^{cre/WT}$ Was floxed (AIDG23S GCBWcKO) and CTL AID$^{G23S/G23S}$ Cγ1$^{cre/WT}$ (AIDG23S CTL) mouse strains. Assessment of anti-dsDNA IgG antibodies in 6-month-old unimmunized animals showed that development of such autoantibodies was totally prevented in AIDG23S GCBWcKO mice (Figure 4D), suggesting that autoimmunity in GCBWcKO mice results from biased selection of poorly mutated PCs.

WASp deficiency reduces GCB apoptosis

Because PCs showed signs of biased selection, we investigated the effects of WASp deletion in GCBs on the cell cycle and apoptosis, two fundamental parameters that regulate GCB progression during the GC reaction. To avoid the confounding asynchronized feature of sptGCs, we performed these experiments in immunized mice. EdU was injected intraperitoneally (i.p.) 1.5 h or 6 h before recovery of splenocytes from hRBC-immunized mice. At the 1.5-h time point, 20.93% ± 2.28% of CTL GCBs appeared to be EdU-labeled compared with 24.10% ± 1.33% of GCBWcKO GCBs. Based on DAPI content, we determined that, in CTL and GCBWcKO mice, respectively, 12.30% ± 2.05% and 13.60% ± 1.75% of the EdU$^+$ GCBs were in early S phase, and 7.05% ± 1.30% and 8.13% ± 0.94% were in late S phase (Figure 5A). 6 h after EdU injection, the percentages of EdU$^+$ cells that had completed their cell cycle and returned to G1 phase (30.60% ± 2.81% versus 30.94% ± 1.05%) or had progressed to G2/M phase (6.26% ± 0.81 versus 6.72% ± 0.24%) and the percentage of recent cycling, EdU$^-$ S-phase cells (5.67% ± 1.55% versus 5.98% ± 1.19%) did not differ significantly between CTL and GCBWcKO GCBs (Figure 5A). Based on these data, we conclude that WASp deficiency in GCBs does not affect the frequency or kinetics of cell cycling. These results are consistent with previously reported findings in the constitutive *Was* KO model (Dahlberg et al., 2015).

Apoptosis of unselected GCBs is a major feature of the GC response. On average, half of GCBs are lost within 5–6 h because of very fast apoptotic kinetics leading to cell fragmentation occurring only 20 min after commencement of apoptosis (Mayer et al., 2017). This prevents accumulation of apoptotic GCBs and accounts for the finding of small percentages (≈5%) of apoptotic GCBs *in situ* in GCs (Mayer et al., 2017). One of the earliest events of apoptosis (intrinsic and extrinsic) is depolarization of the mitochondrial membrane (Zamzami et al., 1995a, 1995b, 1996; Brenner and Kroemer, 2000; Vayssiere et al., 1994). We used tetramethylrhodamine ethyl ester (TMRE) perchlorate labeling to quantify the proportion of depolarized mitochondrion-containing apoptotic cells (Li et al., 2018; De et al., 2018; Crowley et al., 2016; Jayaraman, 2005; Galluzzi et al., 2007). Splenocytes recovered from CTL mice 14 days post immunization (d.p.i.) showed the expected average of 5.11% ± 0.82% of TMRE-negative GCBs, which validated TMRE labeling as a reliable method to assess physiological apoptosis of GCBs. On the other hand, GCBWcKO mice showed a significant reduction in TMRE-negative GCBs (1.91% ± 0.52%). Interestingly, GCBWcKO post-GCBs (YFP$^+$ IgD$^-$ GL7$^-$) also showed a significant reduction in TMRE-negative frequency (6.69% ± 1.31% versus 13.43% ± 2.79%, $p \leq 0.01$) compared with CTL mice (Figure 5B). Evaluation of caspase-3 expression confirmed the presence of significantly lower proportions of apoptotic GCBs from GCBWcKO mice (Figure S3). The reduction in apoptosis in GCBWcKO GCBs correlated with a slight but significant lower membrane expression of FAS (CD95) (CTL, MFI 395 ± 11.5; GCBWcKO, MFI 355.40 ± 12.40; $p \leq 0.01$) (Figure 5C). In addition, GCBWcKO mice showed an increased DZ/LZ ratio (2.1 ± 0.4 versus 3.7 ± 0.6, $p \leq 0.05$) which has been observed consistently in mouse models in which B cell apoptosis is inhibited (Figure 5D; Mayer et al., 2020). These investigations show that WASp deficiency in GCBs does not affect cell cycle kinetics but reduces apoptosis.

WASp deficiency increases PB/PC differentiation

To further characterize the effect of WASp deficiency on GCBs, we performed RNA sequencing (RNA-seq) analysis on YFP$^+$ DZ GCBs purified from sptGCs of CTL and GCBWcKO mice. The large reduction in LZ YFP$^+$ frequency in GCBWcKO mice did not permit us to conduct such an analysis on these cells. A cohort of 233 genes appeared to be significantly dysregulated (Table S2). In line with these findings, this included genes related to apoptosis and, as

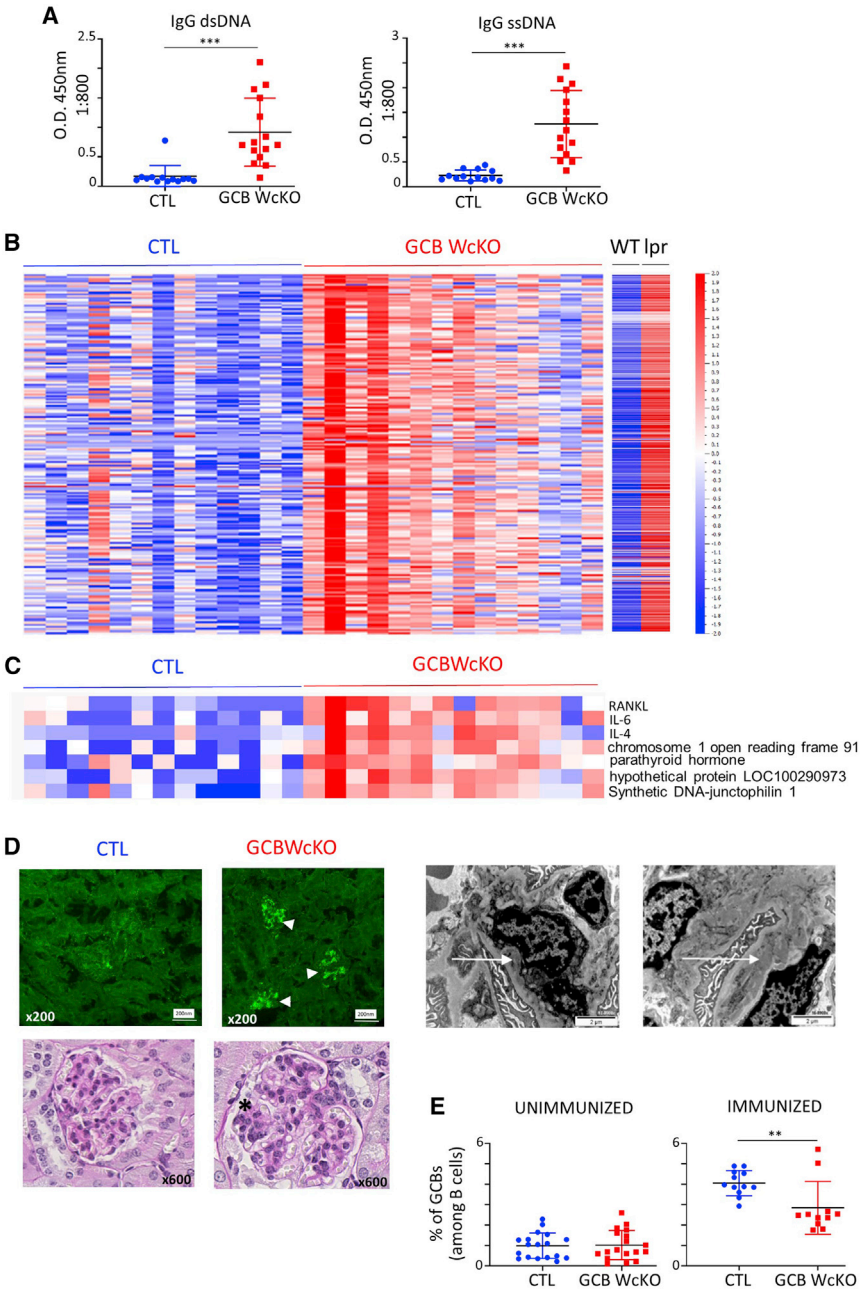

Figure 3. *Was* deletion in GCBs is sufficient to induce autoimmunity

(A) Detection of IgG autoantibody anti-DNA (single-stranded DNA [ssDNA] and double-stranded DNA [dsDNA]), measured by enzyme-linked immunosorbent assay (mean ± SD).

(B and C) Detection of IgG autoantibodies by protein chip array in sera from the indicated mice. Each line represents an antigen (see details in Table S2) and each column a mouse.

(D) Left panels: staining for IgG on frozen OCT-embedded kidney sections revealed glomerular deposits in samples from GCBWcKO mice (white arrowheads) localized in the subendothelial and mesangial space (right panels, white arrows), as revealed by electronic microscopy. Bottom panels: periodic acid-Schiff staining of formalin-fixed, paraffin-embedded kidney sections revealed hypercellularity in samples from GCBWcKO mice (black asterisk). Representative images from analysis of 6 6-month-old mice per group are shown.

(E) Frequency of sptGCs in 6-month-old unimmunized and hRBC-immunized CTL and GCBWcKO mice analyzed at 14 d.p.i.

Statistical significance is indicated on graphs as determined by unpaired Student's t test. **p < 0.01, ***p < 0.001.

expected, actin function (Figure 6A). We performed a gene set enrichment analysis that identified dysregulation of the IL-2_STAT5, mTORC1, and IL-6_JAK_STAT3 signaling pathways (Figure 6B). The IL-2 signaling pathway is implicated in down-regulation of Bach2 in B cells, which, in turn, induces expression of several PB transcription factors (Hipp et al., 2017). Interestingly, Bach2 was significantly downregulated in GCBWcKO GCBs, whereas PB transcription factors, including IRF4 and XBP1, were significantly upregulated, as were several genes associated with cell stress response. This is consistent with the increased endoplasmic reticulum stress and activation of the unfolded protein response associated with PC differentiation (Lam and Bhattacharya, 2018; Figure 6C). To assess whether WASp-deficient GCBs had an increased capacity to differentiate into PCs, we immunized $Cy1^{cre/WT}$ $Was^{lox/WT}$ heterozygous females and analyzed WASp expression in GCBs and PBs/PCs 14d.p.i. Despite a certain degree of heterogeneity, the PB/PC compartment of each analyzed mouse was significantly enriched for WASp-negative cells (30.4% ± 11.4%) compared with the respective GCB compartment (Figure 6D).

Consistent with the observed functional enrichment of the mTORC1 signaling pathway (Caron et al., 2015), we observed a significant increase in uptake of the fatty acid analog BODIPY-FL C12 (C12) by GCBWcKO GCBs (Figure 6E). Conversely, exposure to the glucose analog 2-NBDG did not show differences in frequency and fluorescence intensity of labeled cells from CTL and GCBWcKO GCBs (Figure S4). Given that GCBs selectively oxidize fatty acid over glucose for energy production (Weisel et al., 2020), these findings are in line with the expected increased energy requirements necessary for the massive expansion of the endoplasmic reticulum that characterizes differentiation from GCBs to PCs and sustains immunoglobulin synthesis and secretion (Bertolotti et al., 2010; Lam and Bhattacharya, 2018).

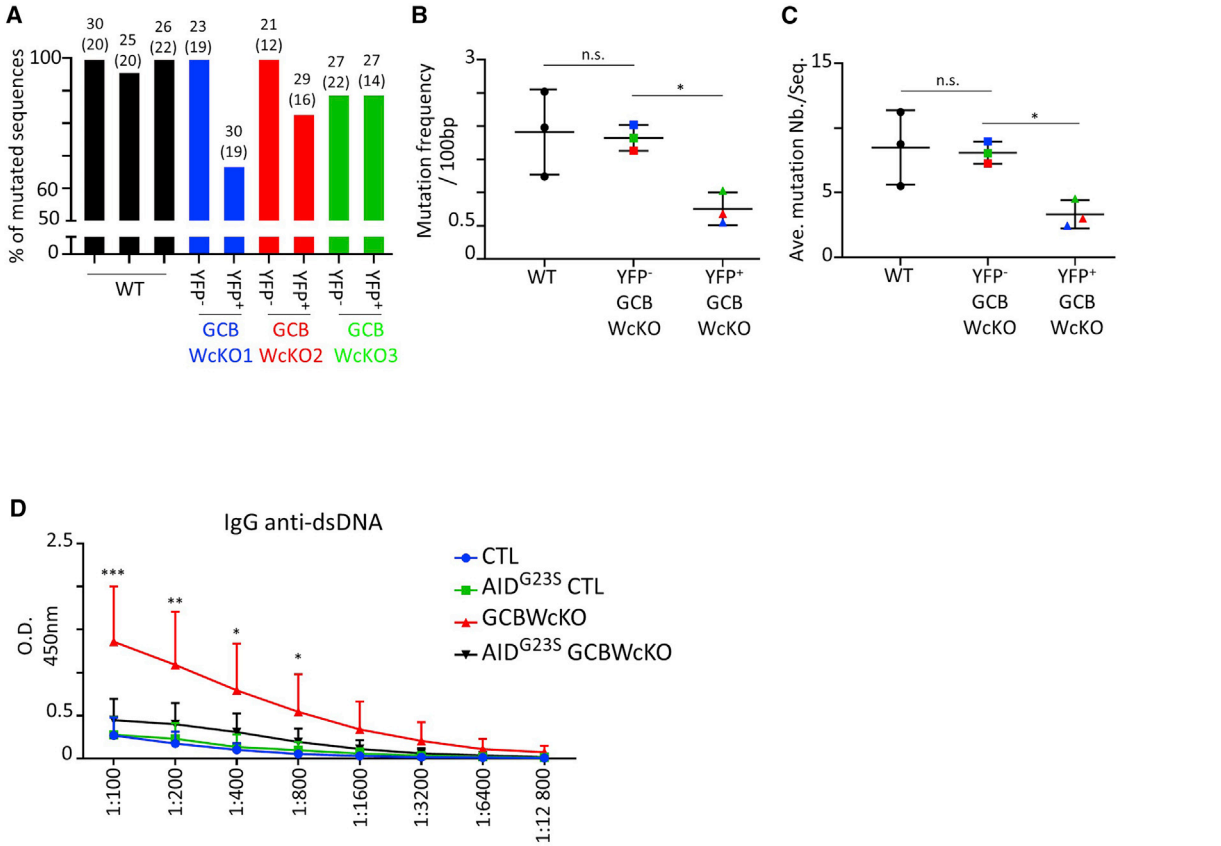

Figure 4. Reduced mutation of Wasp-deficient PCs

(A) Percentage of mutated J_H4 intronic sequences detected in PCs from 6-month-old CTL and *Was*-retaining (YFP^-) and *Was*-deleted (YFP^+) GCBWcKO mice. For each sample, the number of analyzed sequences and the number of identified clones (in brackets) are indicated.

(B) Frequency of mutations detected within J_H4 intronic sequences of PCs from CTL, Was-retaining (YFP^-), and Was-deleted (YFP^+) GCBWcKO mice and expressed as mutations per 100 bp (mean ± SD). Samples obtained from the same mouse are color coded.

(C) Average number of mutations for mutated J_H4 intronic sequences of PCs from CTL, Was-retaining (YFP^-), and Was-deleted mice (YFP^+) GCBWcKO mice (mean ± SD). Samples obtained from the same mouse are color coded.

(D) Detection of IgG anti-dsDNA autoantibodies measured by enzyme-linked immunosorbent assay (mean ± SD).

Pooled data from 3 independent experiments are shown (9–20 mice per group). Statistical analysis (asterisks) corresponds to GCBWcKO versus AID^{G23S} GCBWcKO mice. In (B) and (C), statistical significance was determined using a paired Student's t test (*$p < 0.05$).

Diversification is the main contributor to autoantibody production in *Was* KO mice

Previous investigations have supported the hypothesis that, in *Was* KO as well as in B/WcKO and WBchim mice, autoantibody development is secondary to the presence of a low number of self-reactive naive B cells that escape T cell control and form self-reactive sptGCs (Arkatkar et al., 2017; Jackson et al., 2016; Kolhatkar et al., 2015). Our results suggest that autoantibody-producing clones can originate from a normal pool of naive B cells entering the GC reaction in the absence of increased sptGC development. To relate our observations to the earlier findings, we took advantage of the observation that C57BL/6 mice, but not BALB/c mice, show immunological ignorance for the HEL antigen (Chaouat et al., 1991). We immunized BALB/c and C57BL/6 mice along with aged (6-month-old) *Was* KO mice on the C57BL/6 background with a mixture of HEL and ovalbumin (OVA) antigens. As shown in Figure 7A, all mouse strains showed effective humoral immune responses against OVA. However, similar to the parental C57BL/6 CTL mice, *Was* KO mice showed a lack of antibody response to HEL. Together with prior evidence from the literature indicating that B cell anergy is not affected in the absence of WASp expression (Kolhatkar et al., 2015), these findings are consistent with the peripheral B cell responses remaining T cell-dependent in *Was* KO mice. We then generated $AID^{G23S/G23S}$ *Was* KO mice (AIDG23S *Was* KO) and analyzed the effects of diversification inhibition on the autoimmune features of constitutive *Was* deletion. Unimmunized, 6-month-old *Was* KO and AIDG23S *Was* KO mice showed significantly higher frequencies of sptGCs compared with wild-type (WT) and AIDG23S *Was* WT CTL mice (Figure 7B). However, development of IgG anti-dsDNA antibodies was strongly reduced in AIDG23S *Was* KO compared with *Was* KO mice despite being increased compared with WT and AIDG23S *Was* WT animals (Figure 7C). These results suggest that the main factor resulting in development of autoantibodies in *Was* KO mice is the process of B cell diversification occurring during

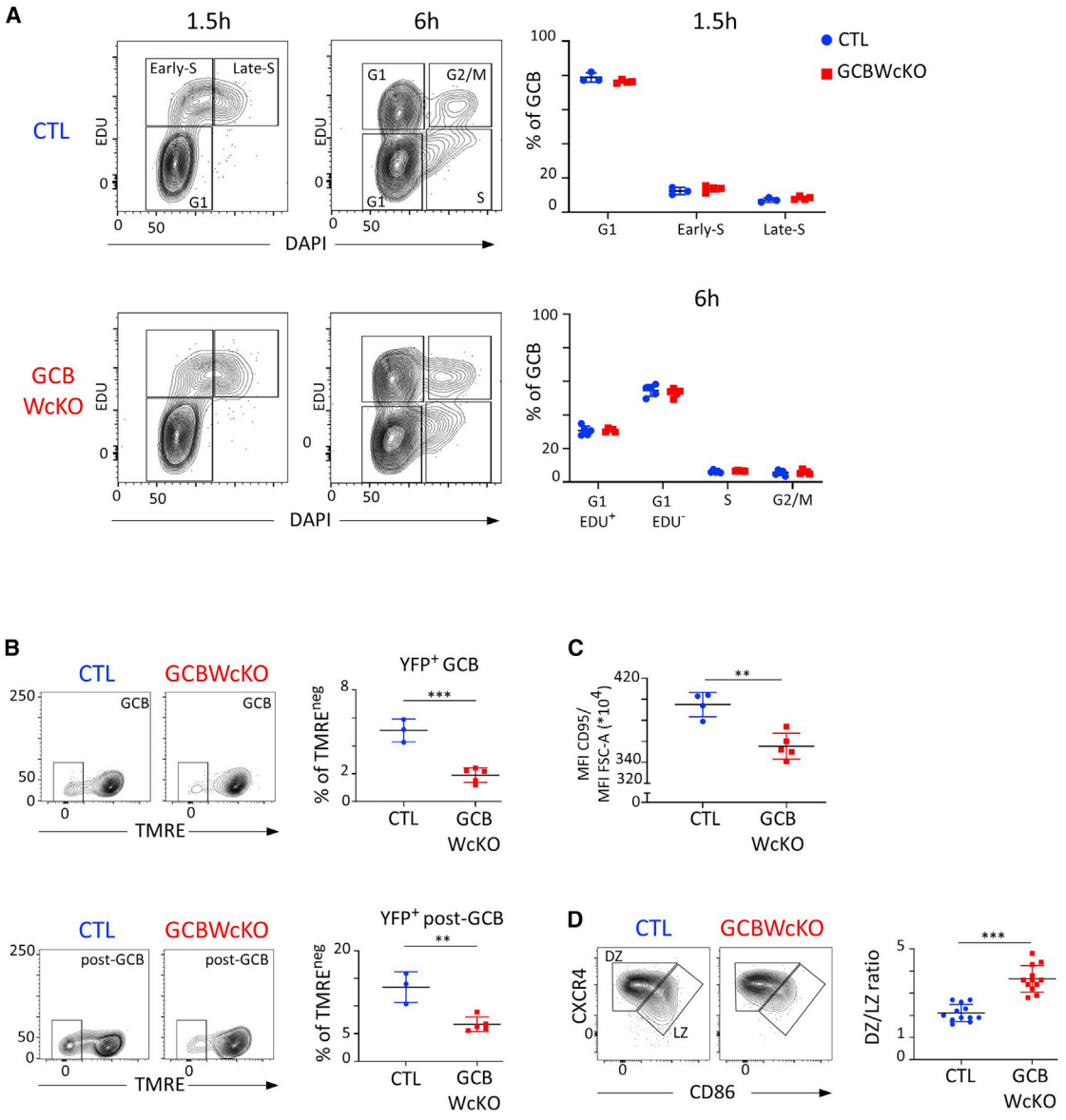

Figure 5. Cell cycle, apoptosis, and DZ/LZ distribution characteristics in GCBWcKO mice

(A) Representative plots showing the distribution of EDU$^-$ and DAPI$^-$ labeled GCBs 1.5 and 6 h after EDU injection. The frequencies of GCBs found in each cell cycle phase are plotted in the right panels (mean ± SD). Data are representative of 2 independent experiments.

(B) Representative flow cytometry plots of TMRE-labeled, YFP$^+$ GCBs and post-GCBs showing TMRE-negative cell gating. Right panels: frequencies of TMRE-negative fractions (mean ± SD). Data are representative of 3 independent experiments.

(C) Mean fluorescence intensity (MFI) of FAS (CD95) expression by living CD19$^+$ GL7$^+$ IgD$^-$ YFP$^+$ GCBs relative to cell size (mean ± SD). Data are representative of 3 independent experiments.

(D) Representative flow cytometry plots of YFP$^+$ GCBs stained for the CXCR4 and CD86 markers to identify the DZ and LZ distribution. Right panel: pooled ratio values of three independent experiments (mean ± SD).

Statistical significance was determined by unpaired Student's t test and is indicated as follows: *p < 0.05, **p < 0.01, ***p < 0.001.

the GC reaction rather than activation of self-reactive, naive B cells.

DISCUSSION

Decades after autoimmune complications were first described in individuals with WAS, the underlying mechanisms remain obscure (Dupuis-Girod et al., 2003). Previous studies have identified intrinsic B cell defects associated with development of autoantibodies in WAS, but at which step B cells break tolerance and by which mechanism(s) still needs to be determined.

Perhaps not unexpectedly, we found that GCBs express high levels of WASp compared with pre- and post-GCBs. This finding is consistent with a primary role of WASp for optimal function of

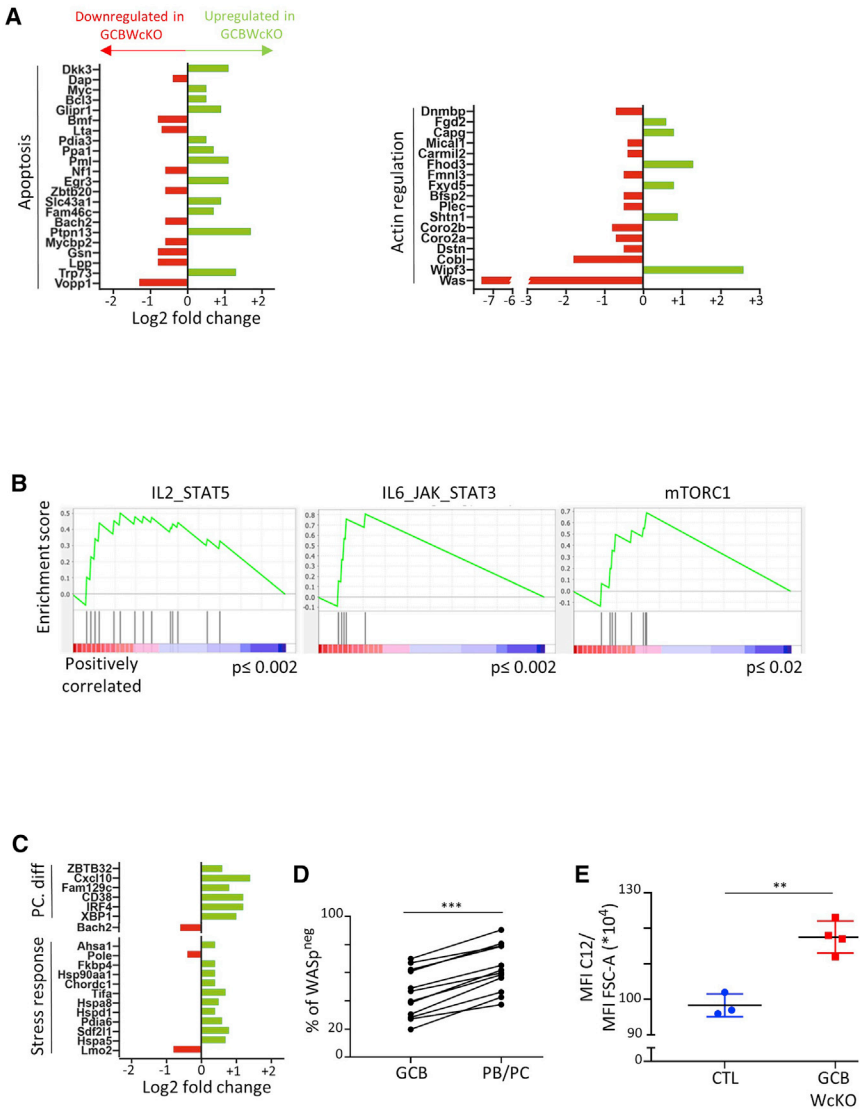

Figure 6. Gene expression patterns and increased PC differentiation program in GCBWcKO mice

(A) Log(2) fold change expression values for significant dysregulated apoptosis- and actin-related genes.

(B) Results of gene set enrichment analysis (GSEA) indicating upregulation of the IL-2_STAT5, IL-6_JAK_STAT3, and mTORC1 pathways. The nominal p values relative to each pathway are indicated.

(C) Log(2) fold change expression values for significant dysregulated PC differentiation (diff.) and stress response-related genes.

(D) Mean frequencies of WASp-negative cells among GCBs and PBs/PCs from heterozygous GCBWcKO female mice. Data are representative of 3 independent experiments. Statistical significance was determined using a paired Student's t test (***$p < 0.001$).

(E) MFI of BODIPY-FL_C12 (C12)-labeled cells relative to cell size (mean ± SD). Data are representative of 2 independent experiments. Statistical significance was determined using an unpaired Student's t test (**$p < 0.01$).

GCBs. A recent study demonstrated the crucial role of WASp in formation, stabilization, and duration of the immunological synapse in GCBs as well as spreading and adhesion of such cells to antigen-presenting surfaces (Li et al., 2021). Despite the notion that GCBs rely on WASp-dependent structures, such as the immunological synapse, to discriminate the affinity of antigen displayed by antigen-presenting cells (Kwak et al., 2018) and capture antigen for processing and presentation (Nowosad et al., 2016) and activation of BCR signaling, whether WASp is required for proper selection of GCBs is still unknown.

Our novel GCB-specific *Was* KO mouse model provided evidence demonstrating unique requirements for WASp in the process of GCB selection. A key finding from our experiments was that unimmunized GCBWcKO mice develop a broad range of autoantibodies. In addition, anti-DNA antibodies and immune complex deposits are already present at 6 months of age, which mirrors the phenotype of the *Was* KO, B/WcKO, and WBchim mice (Becker-Herman et al., 2011; Recher et al., 2012). This is even more notable in the face of the low frequency of Cre recombined (YFP^+) cells observed in unimmunized GCBWcKO mice, which indicates that only ~40% of WASp-deficient GCBs are sufficient to sustain development of autoimmunity. Thus, WASp deficiency in the GC appears to be a strong driver of breach of tolerance.

Similar to other autoimmunity-prone models (Luzina et al., 2001), in *Was* KO and B/WcKO mice, autoimmunity and autoantibodies correlate with increased development of sptGCs, which has been proposed to originate from enrichment of low self-reactive, naive B cells escaping the T cell-mediated enforced tolerance through IL-6 secretion and interferon (INF)-gamma responsiveness (Arkatkar et al., 2017; Jackson et al., 2016; Kolhatkar et al., 2015). However, self-reactivity can also be acquired during the process of B cell diversification (Di Zenzo et al., 2012; Mietzner et al., 2008; Piccoli et al., 2015; Schroeder et al., 2013; Fichtner et al., 2020). We demonstrate here that this is an important mechanism at play in the setting of WASp deficiency. GCBWcKO mice showed an increased DZ/LZ ratio that is a feature of mouse strains in which GCB apoptosis is inhibited (Mayer et al., 2020). The frequency of apoptotic GCBs and post-GCBs is reduced in GCBWcKO mice and correlates with decreased FAS expression. Abundant literature links affinity maturation, selection, and development of self-reactive PCs to regulation of apoptosis in GCs. In general, inhibition of apoptosis in GCBs leads to selection of low-affinity PCs (Takahashi et al., 1999; Wensveen et al., 2012) and production of autoantibodies (Strasser et al., 1991; Bouillet et al., 1999; Takeuchi et al.,

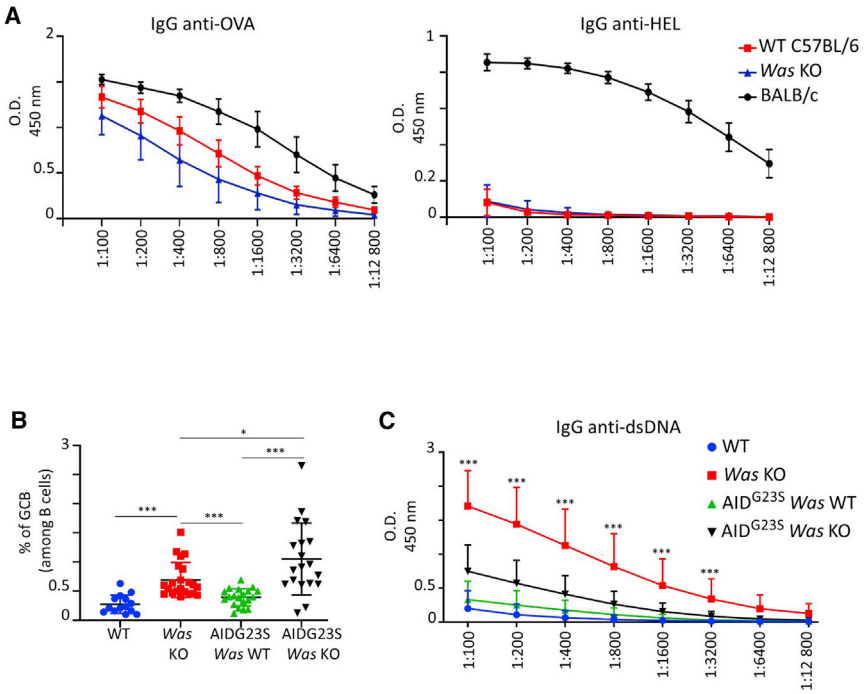

Figure 7. HEL tolerance is functional in *Was* KO mice, and autoantibody development is dependent on diversification

(A) Detection of anti-OVA and anti-HEL IgG antibodies measured by enzyme-linked immunosorbent assay (mean ± SD) in 6 month-old animals immunized i.p. with 100 μg of each antigen in alum. Sera were collected for analysis 12 d.p.i.

(B) Frequencies of sptGCBs ($DAPI^-$ $CD19^+$ $GL7^+$ IgD^- cells) in samples from the indicated mouse strains (6 months old). Pooled results from three independent experiments are shown (mean ± SD).

(C) Detection of anti-dsDNA IgG antibodies measured by enzyme-linked immunosorbent assay (mean ± SD) in 6-month-old animals. Pooled data from 3 independent experiments are shown (14–22 mice per group). Statistical analysis (asterisks) corresponds to *Was* KO versus AID^{G23S} *Was* KO.

Statistical significance was determined using an unpaired Student's t test (*$p < 0.05$, ***$p < 0.001$).

2005). Strikingly, *Fas* deficiency in GCBs has been shown to induce self-reactive PCs with decreased mutation frequency (Butt et al., 2015), a feature shown by *Was*-deficient PCs in our GCBWcKO model and self-reactive V_H4-34 IgM memory cells in individuals with WAS (Kolhatkar et al., 2015). In addition, it has been proposed recently that disruption of apoptosis in post-GCBs results in autoimmunity (Mayer et al., 2020), which is consistent with our results and a role of WASp in post-GCB apoptosis and selection.

Importantly, we demonstrate that diversification is required for autoantibodies to develop in GCBWcKO mice. We hypothesize that the increased capacity of WASp-deficient GCBs to differentiate into PCs leads to incomplete diversification and self-reactivity (Lecerf et al., 2019; Okumura et al., 2012; Tanaka et al., 2017), but we cannot rule out the possibility that alternative mechanisms leading to a dysfunctional GC, as reflected by the abnormal DL/LZ ratio, may also affect the normal selection process of the remaining WASp-expressing counterparts.

Consistent with the importance of IL-6 for development of autoimmunity in BWchim models (Arkatkar et al., 2017), we found that genes involved in the IL-6_STAT3 pathway were enriched in WASp-deficient GCBs. Thus, our findings point to the GC reaction as an important point where B cell-derived IL-6 is likely to play a role.

Another main observation from our experiments is that the non-responsiveness to the HEL antigen is preserved in *Was* KO mice. T cell transfer experiments have indicated previously that this phenomenon is mediated, at least in part, by T cell suppression (Adorini et al., 1979). These findings therefore raise the question of whether the role of WASp in Treg cell-mediated suppression of self-reactive B cell activation we have demonstrated previously in *in vitro* experiments (Adriani et al., 2011) is relevant to the *in vivo* setting. As observed in MRL/lpr mice (Hao et al., 2018), prevention of GCB diversification in *Was* KO animals markedly reduced development of anti-DNA antibodies in the presence of an increased frequency of sptGCs. This suggests that WASp-deficient sptGCs are largely of a non-self-reactive nature and that the emergence of self-reactive GCBs during diversification is the main mechanism leading to autoimmunity in *Was* KO mice.

Recently, isotype switching has been shown to take place very early after initial B cell/T cell interactions and before initiation of the GC (Roco et al., 2019). Because our experiments did not establish a direct link between WASp-deficient BM long-lived PCs and production of autoantibodies, we cannot exclude the possibility that, in our GCBWcKO model, self-reactive clones derive from extrafollicular reactions. This possibility has not yet been investigated in WASp-deficient models, but our data suggest that such extrafollicular production would still require diversification for self-reactivity to emerge (William et al., 2002).

Based on prior evidence from the literature and our findings, we propose a model where the increased development of sptGCs in the *Was* KO, B/WcKO, or WBchim models results from a hyperactivation state of naive B cells because of increased BCR and Toll-like receptor (TLR) signaling (Kolhatkar et al., 2015; Pala et al., 2015). These sptGCs are likely of a non-self-reactive nature because of preserved T cell dependency of *Was* KO B cell responses. However, the increased prevalence of sptGCs may lead to emergence of more GCBs that acquire self-reactivity through incomplete diversification. Such cells feature an increased survival capacity, allowing them to escape selection and differentiate into PCs, leading to autoimmunity, mirroring the mechanisms active in systemic lupus erythematosus in humans (Cappione et al., 2005). These observations may justify clinical investigation of alternative therapies for autoimmunity based on agents specifically targeting PCs (e.g., the anti-CD38 monoclonal antibody daratumumab)

to modulate the abnormal immunological tolerance processes that affect individuals with WAS.

Limitations of the study

Although use of mouse genetics allows dissection of specific aspects of the role of WASp in the differentiation and function of GCB cells, these studies may not accurately reflect the totality of mechanisms at play in humans affected with WAS, where residual levels of WASp expression are common and WASp-defective B cells interact with WASp-defective T cells during the critical process of the GC reaction and SHM.

STAR★METHODS

Detailed methods are provided in the online version of this paper and include the following:

- KEY RESOURCES TABLE
- RESOURCE AVAILABILITY
  - Lead contact
  - Materials availability
  - Data and code availability
- METHOD DETAILS
  - Mice and immunizations
  - Cells preparation for FACS and intracellular staining
  - RNA-seq
  - TMRE, 2-NBDG and BODIPY-FL-C12 labeling
  - CHIP array
  - ELISA
  - J_H4 intron sequence mutation analysis
  - Cell cycle analysis
  - Histological analysis
- QUANTIFICATION AND STATISTICAL ANALYSIS

SUPPLEMENTAL INFORMATION

Supplemental information can be found online at https://doi.org/10.1016/j.celrep.2022.110474.

ACKNOWLEDGMENTS

We thank the staff of the animal facility of Epalinges, Switzerland for excellent daily and humane care of our mice; Alba de los Aires for precious help with J_h4 sequence analysis; Dr. Sandra Weller, Dr. Sebastien Storck, and Clara Cousu for helpful discussions; Ms. Blerta Kicaj for the graphical abstract realization; Ms. Janine Horlbeck for excellent technical help; and Dr. Reiko Shinkura for facilitating transfer of the AIDG23S mice. This project was supported by grant 310030-179251 from the Suisse National Science Foundation (SNF) (to F.C.), funds from the BLACKSWAN Foundation (BSF-005) (to M.D.), and the Wellcome Trust (to A.J.T.).

AUTHOR CONTRIBUTIONS

Conceptualization, M.D.; methodology, M.D.; investigation, M.D., R.F., S.R., S.D.-G., G.K., X.C.L., and E.T.; funding acquisition, M.D. and F.C.; supervision, F.C.; writing – original draft, M.D. and F.C.; writing – review & editing, M.D., F.C., and A.J.T.

DECLARATION OF INTERESTS

The authors declare no competing interests.

Received: April 7, 2021
Revised: August 18, 2021
Accepted: February 10, 2022
Published: March 8, 2022

REFERENCES

Adorini, L., Harvey, M.A., Miller, A., and Sercarz, E.E. (1979). Fine specificity of regulatory T cells. II. Suppressor and helper T cells are induced by different regions of hen egg-white lysozyme in a genetically nonresponder mouse strain. J. Exp. Med. *150*, 293–306.

Adriani, M., Jones, K.A., Uchiyama, T., Kirby, M.R., Silvin, C., Anderson, S.M., and Candotti, F. (2011). Defective inhibition of B-cell proliferation by Wiskott-Aldrich syndrome protein-deficient regulatory T cells. Blood *117*, 6608–6611.

Arkatkar, T., DU, S.W., Jacobs, H.M., Dam, E.M., hou, B., Buckner, J.H., Rawlings, D.J., and Jackson, S.W. (2017). B cell-derived IL-6 initiates spontaneous germinal center formation during systemic autoimmunity. J. Exp. Med. *214*, 3207–3217.

Becker-Herman, S., Meyer-Bahlburg, A., Schwartz, M.A., Jackson, S.W., Hudkins, K.L., Liu, C., Sather, B.D., Khim, S., Liggitt, D., Song, W., et al. (2011). WASp-deficient B cells play a critical, cell-intrinsic role in triggering autoimmunity. J. Exp. Med. *208*, 2033–2042.

Bertolotti, M., Yim, S.H., Garcia-Manteiga, J.M., Masciarelli, S., Kim, Y.J., Kang, M.H., Iuchi, Y., Fujii, J., Vené, R., Rubartelli, A., et al. (2010). B- to plasma-cell terminal differentiation entails oxidative stress and profound reshaping of the antioxidant responses. Antioxid. Redox Signal. *13*, 1133–1144.

Bosticardo, M., Marangoni, F., Aiuti, A., Villa, A., and Grazia Roncarolo, M. (2009). Recent advances in understanding the pathophysiology of Wiskott-Aldrich syndrome. Blood *113*, 6288–6295.

Bouillet, P., Metcalf, D., Huang, D.C., Tarlinton, D.M., Kay, T.W., Köntgen, F., Adams, J.M., and Strasser, A. (1999). Proapoptotic Bcl-2 relative Bim required for certain apoptotic responses, leukocyte homeostasis, and to preclude autoimmunity. Science *286*, 1735–1738.

Brenner, C., and Kroemer, G. (2000). Apoptosis. Mitochondria–the death signal integrators. Science *289*, 1150–1151.

Bretscher, P., and Cohn, M. (1970). A theory of self-nonself discrimination. Science *169*, 1042–1049.

Burnett, D.L., Langley, D.B., Schofield, P., Hermes, J.R., Chan, T.D., Jackson, J., Bourne, K., Reed, J.H., Patterson, K., Porebski, B.T., et al. (2018). Germinal center antibody mutation trajectories are determined by rapid self/foreign discrimination. Science *360*, 223–226.

Butt, D., Chan, T.D., Bourne, K., Hermes, J.R., Nguyen, A., Statham, A., O'reilly, L.A., Strasser, A., Price, S., Schofield, P., et al. (2015). FAS inactivation releases unconventional germinal center B cells that escape antigen control and drive IgE and autoantibody production. Immunity *42*, 890–902.

Cambier, J.C., Gauld, S.B., Merrell, K.T., and Vilen, B.J. (2007). B-cell anergy: from transgenic models to naturally occurring anergic B cells? Nat. Rev. Immunol. *7*, 633–643.

Candotti, F. (2018). Clinical manifestations and pathophysiological mechanisms of the wiskott-aldrich syndrome. J. Clin. Immunol. *38*, 13–27.

Cappione, A., 3rd, Anolik, J.H., Pugh-Bernard, A., Barnard, J., Dutcher, P., Silverman, G., and Sanz, I. (2005). Germinal center exclusion of autoreactive B cells is defective in human systemic lupus erythematosus. J. Clin. Invest. *115*, 3205–3216.

Caron, A., Richard, D., and Laplante, M. (2015). The roles of mTOR complexes in lipid metabolism. Annu. Rev. Nutr. *35*, 321–348.

Casola, S., Cattoretti, G., Uyttersprot, N., Koralov, S.B., Seagal, J., Hao, Z., Waisman, A., Egert, A., Ghitza, D., and Rajewsky, K. (2006). Tracking germinal center B cells expressing germ-line immunoglobulin gamma1 transcripts by conditional gene targeting. Proc. Natl. Acad. Sci. U S A *103*, 7396–7401.

Chan, T.D., Wood, K., Hermes, J.R., Butt, D., Jolly, C.J., Basten, A., and Brink, R. (2012). Elimination of germinal-center-derived self-reactive B cells is governed by the location and concentration of self-antigen. Immunity *37*, 893–904.

Chaouat, G., Kinsky, R., Hofmann, R., Combe, C.R., and Kourilsky, P. (1991). The in vivo antibody response to hen egg white lysozyme in H-2b-compatible responder and non-responder mice: is it regulated by its N-terminal peptide at the level of antigen-presenting cells? Res. Immunol. *142*, 799–813.

Crowley, L.C., Christensen, M.E., and Waterhouse, N.J. (2016). Measuring mitochondrial transmembrane potential by TMRE staining. Cold Spring Harb. Protoc. *2016*. https://doi.org/10.1101/pdb.prot087361.

Dahlberg, C.I., Torres, M.L., Petersen, S.H., Baptista, M.A., Keszei, M., Volpi, S., Grasset, E.K., Karlsson, M.C., Walter, J.E., Snapper, S.B., et al. (2015). Deletion of WASp and N-WASp in B cells cripples the germinal center response and results in production of IgM autoantibodies. J. Autoimmun. *62*, 81–92.

De, P., Carlson, J.H., Leyland-Jones, B., Williams, C., and Dey, N. (2018). Triple fluorescence staining to evaluate mechanism-based apoptosis following chemotherapeutic and targeted anti-cancer drugs in live tumor cells. Sci. Rep. *8*, 13192.

Di Zenzo, G., Di Lullo, G., Corti, D., Calabresi, V., Sinistro, A., Vanzetta, F., Didona, B., Cianchini, G., Hertl, M., Eming, R., et al. (2012). Pemphigus autoantibodies generated through somatic mutations target the desmoglein-3 cis-interface. J. Clin. Invest. *122*, 3781–3790.

Dupuis-Girod, S., Medioni, J., Haddad, E., Quartier, P., Cavazzana-Calvo, M., Le Deist, F., De Saint Basile, G., Delaunay, J., Schwarz, K., Casanova, J.L., et al. (2003). Autoimmunity in Wiskott-Aldrich syndrome: risk factors, clinical features, and outcome in a single-center cohort of 55 patients. Pediatrics *111*, e622–e627.

Fichtner, M.L., Vieni, C., Redler, R.L., Kolich, L., Jiang, R., Takata, K., Stathopoulos, P., Suarez, P.A., Nowak, R.J., Burden, S.J., et al. (2020). Affinity maturation is required for pathogenic monovalent IgG4 autoantibody development in myasthenia gravis. J. Exp. Med. *217*, e20200513.

Galluzzi, L., Zamzami, N., De La Motte Rouge, T., Lemaire, C., Brenner, C., and Kroemer, G. (2007). Methods for the assessment of mitochondrial membrane permeabilization in apoptosis. Apoptosis *12*, 803–813.

Hao, F., Tian, M., Feng, Y., Quan, C., Chen, Y., Chen, S., and Wei, M. (2018). Abrogation of lupus nephritis in somatic hypermutation-deficient MRL/lpr mice. J. Immunol. *200*, 3905–3912.

He, M., and Westerberg, L.S. (2019). Congenital defects in actin dynamics of germinal center B cells. Front. Immunol. *10*, 296.

Hipp, N., Symington, H., Pastoret, C., Caron, G., Monvoisin, C., Tarte, K., Fest, T., and Delaloy, C. (2017). IL-2 imprints human naive B cell fate towards plasma cell through ERK/ELK1-mediated BACH2 repression. Nat. Commun. *8*, 1443.

Humblet-Baron, S., Sather, B., Anover, S., Becker-Herman, S., Kasprowicz, D.J., Khim, S., Nguyen, T., Hudkins-Loya, K., Alpers, C.E., Ziegler, S.F., et al. (2007). Wiskott-Aldrich syndrome protein is required for regulatory T cell homeostasis. J. Clin. Invest. *117*, 407–418.

Jackson, S.W., Jacobs, H.M., Arkatkar, T., Dam, E.M., Scharping, N.E., Kolhatkar, N.S., Hou, B., Buckner, J.H., and Rawlings, D.J. (2016). B cell IFN-γ receptor signaling promotes autoimmune germinal centers via cell-intrinsic induction of BCL-6. J. Exp. Med. *213*, 733–750.

Jayaraman, S. (2005). Flow cytometric determination of mitochondrial membrane potential changes during apoptosis of T lymphocytic and pancreatic beta cell lines: comparison of tetramethylrhodamineethylester (TMRE), chloromethyl-X-rosamine (H2-CMX-Ros) and MitoTracker Red 580 (MTR580). J. Immunol. Methods *306*, 68–79.

Kelly, A.E., Kranitz, H., Dötsch, V., and Mullins, R.D. (2006). Actin binding to the central domain of WASP/Scar proteins plays a critical role in the activation of the Arp2/3 complex. J. Biol. Chem. *281*, 10589–10597.

Kolhatkar, N.S., Brahmandam, A., Thouvenel, C.D., Becker-Herman, S., Jacobs, H.M., Schwartz, M.A., Allenspach, E.J., Khim, S., Panigrahi, A.K., Luning Prak, E.T., et al. (2015). Altered BCR and TLR signals promote enhanced positive selection of autoreactive transitional B cells in Wiskott-Aldrich syndrome. J. Exp. Med. *212*, 1663–1677.

Kwak, K., Quizon, N., Sohn, H., Saniee, A., Manzella-Lapeira, J., Holla, P., Brzostowski, J., Lu, J., Xie, H., Xu, C., et al. (2018). Intrinsic properties of human germinal center B cells set antigen affinity thresholds. Sci. Immunol. *3*, eaau6598.

Lam, W.Y., and Bhattacharya, D. (2018). Metabolic links between plasma cell survival, secretion, and stress. Trends Immunol. *39*, 19–27.

Le Gallou, S., Zhou, Z., Thai, L.H., Fritzen, R., De Los Aires, A.V., Mégret, J., Yu, P., Kitamura, D., Bille, E., Tros, F., et al. (2018). A splenic IgM memory subset with antibacterial specificities is sustained from persistent mucosal responses. J. Exp. Med. *215*, 2035–2053.

Lecerf, M., Kanyavuz, A., Lacroix-Desmazes, S., and Dimitrov, J.D. (2019). Sequence features of variable region determining physicochemical properties and polyreactivity of therapeutic antibodies. Mol. Immunol. *112*, 338–346.

Li, B., Dou, S.X., Yuan, J.W., Liu, Y.R., Li, W., Ye, F., Wang, P.Y., and Li, H. (2018). Intracellular transport is accelerated in early apoptotic cells. Proc. Natl. Acad. Sci. U S A *115*, 12118–12123.

Li, Y., Bhanja, A., Upadhyaya, A., Zhao, X., and Song, W. (2021). WASp is crucial for the unique architecture of the immunological synapse in germinal center B-cells. Front. Cell Dev Biol *9*, 646077.

Luzina, I.G., Atamas, S.P., Storrer, C.E., Dasilva, L.C., Kelsoe, G., Papadimitriou, J.C., and Handwerger, B.S. (2001). Spontaneous formation of germinal centers in autoimmune mice. J. Leukoc. Biol. *70*, 578–584.

Mayer, C.T., Gazumyan, A., Kara, E.E., Gitlin, A.D., Golijanin, J., Viant, C., Pai, J., Oliveira, T.Y., Wang, Q., Escolano, A., et al. (2017). The microanatomic segregation of selection by apoptosis in the germinal center. Science *358*, eaao2602.

Mayer, C.T., Nieke, J.P., Gazumyan, A., Cipolla, M., Wang, Q., Oliveira, T.Y., Ramos, V., Monette, S., LI, Q.Z., Gershwin, M.E., et al. (2020). An apoptosis-dependent checkpoint for autoimmunity in memory B and plasma cells. Proc. Natl. Acad. Sci. U S A *117*, 24957–24963.

Mietzner, B., Tsuiji, M., Scheid, J., Velinzon, K., Tiller, T., Abraham, K., Gonzalez, J.B., Pascual, V., Stichweh, D., Wardemann, H., and Nussenzweig, M.C. (2008). Autoreactive IgG memory antibodies in patients with systemic lupus erythematosus arise from nonreactive and polyreactive precursors. Proc. Natl. Acad. Sci. U S A *105*, 9727–9732.

Muramatsu, M., Kinoshita, K., Fagarasan, S., Yamada, S., Shinkai, Y., and Honjo, T. (2000). Class switch recombination and hypermutation require activation-induced cytidine deaminase (AID), a potential RNA editing enzyme. Cell *102*, 553–563.

Nemazee, D. (2017). Mechanisms of central tolerance for B cells. Nat. Rev. Immunol. *17*, 281–294.

Nowosad, C.R., Spillane, K.M., and Tolar, P. (2016). Germinal center B cells recognize antigen through a specialized immune synapse architecture. Nat. Immunol. *17*, 870–877.

Okumura, F., Sakuma, H., Nakazawa, T., Hayashi, K., Naitoh, I., Miyabe, K., Yoshida, M., Yamashita, H., Ohara, H., Inagaki, H., and Joh, T. (2012). Analysis of VH gene rearrangement and somatic hypermutation in type 1 autoimmune pancreatitis. Pathol. Int. *62*, 318–323.

Pala, F., Morbach, H., Castiello, M.C., Schickel, J.N., Scaramuzza, S., Chamberlain, N., Cassani, B., Glauzy, S., Romberg, N., Candotti, F., et al. (2015). Lentiviral-mediated gene therapy restores B cell tolerance in Wiskott-Aldrich syndrome patients. J. Clin. Invest. *125*, 3941–3951.

Piccoli, L., Campo, I., Fregni, C.S., Rodriguez, B.M., Minola, A., Sallusto, F., Luisetti, M., Corti, D., and Lanzavecchia, A. (2015). Neutralization and clearance of GM-CSF by autoantibodies in pulmonary alveolar proteinosis. Nat. Commun. *6*, 7375.

Recher, M., Burns, S.O., De La Fuente, M.A., Volpi, S., Dahlberg, C., Walter, J.E., Moffitt, K., Mathew, D., Honke, N., Lang, P.A., et al. (2012). B cell-intrinsic deficiency of the Wiskott-Aldrich syndrome protein (WASp) causes severe abnormalities of the peripheral B-cell compartment in mice. Blood *119*, 2819–2828.

Revy, P., Muto, T., Levy, Y., Geissmann, F., Plebani, A., Sanal, O., Catalan, N., Forveille, M., Dufourcq-Labelouse, R., Gennery, A., et al. (2000).

Activation-induced cytidine deaminase (AID) deficiency causes the autosomal recessive form of the Hyper-IgM syndrome (HIGM2). Cell *102*, 565–575.

Roco, J.A., Mesin, L., Binder, S.C., Nefzger, C., Gonzalez-Figueroa, P., Canete, P.F., Ellyard, J., Shen, Q., Robert, P.A., Cappello, J., et al. (2019). Class-switch recombination occurs infrequently in germinal centers. Immunity *51*, 337–350.e7.

Schroeder, K., Herrmann, M., and Winkler, T.H. (2013). The role of somatic hypermutation in the generation of pathogenic antibodies in SLE. Autoimmunity *46*, 121–127.

Shinkura, R., Ito, S., Begum, N.A., Nagaoka, H., Muramatsu, M., Kinoshita, K., Sakakibara, Y., Hijikata, H., and Honjo, T. (2004). Separate domains of AID are required for somatic hypermutation and class-switch recombination. Nat. Immunol. *5*, 707–712.

Snapper, S.B., Rosen, F.S., Mizoguchi, E., Cohen, P., Khan, W., Liu, C.H., Hagemann, T.L., Kwan, S.P., Ferrini, R., Davidson, L., et al. (1998). Wiskott-Aldrich syndrome protein-deficient mice reveal a role for WASP in T but not B cell activation. Immunity *9*, 81–91.

Strasser, A., Whittingham, S., Vaux, D.L., Bath, M.L., Adams, J.M., Cory, S., and Harris, A.W. (1991). Enforced BCL2 expression in B-lymphoid cells prolongs antibody responses and elicits autoimmune disease. Proc. Natl. Acad. Sci. U S A *88*, 8661–8665.

Takahashi, Y., Cerasoli, D.M., Dal Porto, J.M., Shimoda, M., Freund, R., Fang, W., Telander, D.G., Malvey, E.N., Mueller, D.L., Behrens, T.W., and Kelsoe, G. (1999). Relaxed negative selection in germinal centers and impaired affinity maturation in bcl-xL transgenic mice. J. Exp. Med. *190*, 399–410.

Takeuchi, O., Fisher, J., Suh, H., Harada, H., Malynn, B.A., and Korsmeyer, S.J. (2005). Essential role of BAX,BAK in B cell homeostasis and prevention of autoimmune disease. Proc. Natl. Acad. Sci. U S A *102*, 11272–11277.

Tanaka, T., Zhang, W., Sun, Y., Shuai, Z., Chida, A.S., Kenny, T.P., Yang, G.X., Sanz, I., Ansari, A., Bowlus, C.L., et al. (2017). Autoreactive monoclonal antibodies from patients with primary biliary cholangitis recognize environmental xenobiotics. Hepatology *66*, 885–895.

Tiller, T., Tsuiji, M., Yurasov, S., Velinzon, K., Nussenzweig, M.C., and Wardemann, H. (2007). Autoreactivity in human IgG+ memory B cells. Immunity *26*, 205–213.

Vayssiere, J.L., Petit, P.X., Risler, Y., and Mignotte, B. (1994). Commitment to apoptosis is associated with changes in mitochondrial biogenesis and activity in cell lines conditionally immortalized with simian virus 40. Proc. Natl. Acad. Sci. U S A *91*, 11752–11756.

Wardemann, H., Yurasov, S., Schaefer, A., Young, J.W., Meffre, E., and Nussenzweig, M.C. (2003). Predominant autoantibody production by early human B cell precursors. Science *301*, 1374–1377.

Wei, M., Shinkura, R., Doi, Y., Maruya, M., Fagarasan, S., and Honjo, T. (2011). Mice carrying a knock-in mutation of Aicda resulting in a defect in somatic hypermutation have impaired gut homeostasis and compromised mucosal defense. Nat. Immunol. *12*, 264–270.

Weisel, F.J., Mullett, S.J., Elsner, R.A., Menk, A.V., Trivedi, N., Luo, W., Wikenheiser, D., Hawse, W.F., Chikina, M., Smita, S., et al. (2020). Germinal center B cells selectively oxidize fatty acids for energy while conducting minimal glycolysis. Nat. Immunol. *21*, 331–342.

Wensveen, F.M., Derks, I.A., Van Gisbergen, K.P., De Bruin, A.M., Meijers, J.C., Yigittop, H., Nolte, M.A., Eldering, E., and Van Lier, R.A. (2012). BH3-only protein Noxa regulates apoptosis in activated B cells and controls high-affinity antibody formation. Blood *119*, 1440–1449.

Westerberg, L., Larsson, M., Hardy, S.J., Fernandez, C., Thrasher, A.J., and Severinson, E. (2005). Wiskott-Aldrich syndrome protein deficiency leads to reduced B-cell adhesion, migration, and homing, and a delayed humoral immune response. Blood *105*, 1144–1152.

William, J., Euler, C., Christensen, S., and Shlomchik, M.J. (2002). Evolution of autoantibody responses via somatic hypermutation outside of germinal centers. Science *297*, 2066–2070.

Zamzami, N., Marchetti, P., Castedo, M., Decaudin, D., Macho, A., Hirsch, T., Susin, S.A., Petit, P.X., Mignotte, B., and Kroemer, G. (1995a). Sequential reduction of mitochondrial transmembrane potential and generation of reactive oxygen species in early programmed cell death. J. Exp. Med. *182*, 367–377.

Zamzami, N., Marchetti, P., Castedo, M., Zanin, C., Vayssière, J.L., Petit, P.X., and Kroemer, G. (1995b). Reduction in mitochondrial potential constitutes an early irreversible step of programmed lymphocyte death in vivo. J. Exp. Med. *181*, 1661–1672.

Zamzami, N., Susin, S.A., Marchetti, P., Hirsch, T., Gómez-Monterrey, I., Castedo, M., and Kroemer, G. (1996). Mitochondrial control of nuclear apoptosis. J. Exp. Med. *183*, 1533–1544.

STAR★METHODS

KEY RESOURCES TABLE

REAGENT or RESOURCE	SOURCE	IDENTIFIER
Antibodies		
CD19 PeCy7	invitrogen	25-0193-82; RRID:AB_657663
CD19 PrCPCy5.5	BD	551001; RRID:AB_394004
CD19 APC-Fire750	Biolegend	115557; RRID:AB_2572119
IgD Pacific blue	Southern Biotech	1120-26; RRID:AB_2794612
IgD APC-Fire750	Biolegend	405743; RRID:AB_2629765
IgD Pe	BD	558597; RRID:AB_647211
IgD Alexa 700	invitrogen	56-5993-80; RRID:AB_2815255
IgM PrCPCy5.5	Biolegend	406511; RRID:AB_2075944
IgM Pe	Biolegend	406507; RRID:AB_315057
CD95 Pe	BD	554258; RRID:AB_395330
GL7 Pacific blue	Biolegend	144614; RRID:AB_2563292
GL7 Alexa 647	Biolegend	144605; RRID:AB_2562184
CD138 Pacific Blue	Biolegend	142507; RRID:AB_11204257
CXCR4 Pe	invitrogen	12-9991-82; RRID:AB_891391
CXCR4 Pe	Biolegend	146506; RRID:AB_2562783
CXCR4 PrCPCy5.5	Biolegend	146509; RRID:AB_2562786
CD86 PrCPCy5.5	Biolegend	105027; RRID:AB_893420
CD86 Alexa 647	Biolegend	105020; RRID:AB_493464
B220 Pe	ebioscience	12-0452-81; RRID:AB_465670
goat anti-mouse IgG	SouthernBiotech	1033-30; RRID:AB_2794334
anti-mouse IgG-HRP antibodies	SouthernBiotech	1033-05; RRID:AB_2737432
WASp Alexa 647	Santa Cruz	sc-13139; RRID:AB_628445
Chemicals, peptides, and recombinant proteins		
dsDNA	SigmaAldrich	D1626
BODIPY-FL-C12	Invitrogen	D3822
2-NBDG	ThermoFisher	N13195
TMRE	SigmaAldrich	87917
ssDNA	SigmaAldrich	D8899
Ovalbumine	SigmaAldrich	LS003056
Hen Egg Lysozyme	SigmaAldrich	L6876
Critical commercial assays		
Click-It Plus EdU Alexa Fluor 647	Invitrogen	C10634
Reacti-Bind DNA coating solution	Thermo Scientific	17250
Deposited data		
RNA-seq	e ArrayExpress database at EMBL-EBI	E-MTAB-10056
Experimental models: Organisms/strains		
BALB/c	Charles Rivers	N/A
Cy1cre	JAX	010612
AIDG23S	RIKEN	SA9436
Was KO	JAX	019458
C57BL/6	Charles Rivers	N/A

(*Continued on next page*)

Continued		
REAGENT or RESOURCE	SOURCE	IDENTIFIER
Oligonucleotides		
V_H3: 5′-GAGGACACACCCACATATTACTG-3’	Microsynth	N/A
V_H5: 5′-GAGGACACRGCCATGTATTACTG-3′	Microsynth	N/A
V_H6: 5′-GAAGACACTGGAA TTTATTACTG-3′	Microsynth	N/A
V_H7: 5′-GAGGACAGTGCCACTTATTACTG-3′	Microsynth	N/A
V_H9: 5′-ATGAGGACATGG CTACATATTTC-3′	Microsynth	N/A
V_H10/12: 5′-GAGGACACAGCCATGTATTACTG-3′	Microsynth	N/A
V_H11: 5′-GAGGACACAGCCACGTATTTCTG-5′	Microsynth	N/A
J_H4rev: 5′-CACCAGACCTCTCTAGACAGC-3′	Microsynth	N/A
J_H4-nested: 5′-TGAGACCGAGGCTAGATGCC-3′	Microsynth	N/A
V_H1: 5′-GAGGACTCTGCRGTCTATTWCTG-3′	Microsynth	N/A
Software and algorithms		
Prism	graphpad.com	N/A
FlowJo	flowjo.com	N/A

RESOURCE AVAILABILITY

Lead contact

Further information and requests for resources and reagents should be directed to and will be fulfilled by the lead contact, Marc Descatoire (Marc.Descatoire@chuv.ch)

Materials availability

Mouse lines generated in this study are available through the lead contact, Marc Descatoire (Marc.Descatoire@chuv.ch)

Data and code availability

- RNA-seq data have been deposited in the ArrayExpress database at EMBL-EBI under accession number E-MTAB-10056 (https://www.ebi.ac.uk/arrayexpress/experiments/E-MTAB-10056/). Username: Reviewer_E-MTAB-10056; Password: 7nhcccip
- This paper does not report original code.
- Any additional information required to reanalyze the data reported in this work paper is available from the Lead Contact upon request.

METHOD DETAILS

Mice and immunizations

WT C57BL/6 and BALB/c mice were purchased from Charles Rivers (Lyon, France). All *Was*-deficient models were bred on a C57BL/6 background. The generation of Cy1cre, AIDG23S, *Was* KO and *Was* floxed mice has been previously described (Casola et al., 2006; Wei et al., 2011; Snapper et al., 1998; Recher et al., 2012). Mice were used for experiments at different ages as specified. For immunization, mice were injected i.p. with 2×10^9 human red blood cells (hRBC) purchased from the Interregional Blood Transfusion SRC Ltd (Epalinges, CH) with same boosts at day 4 and day 8 before analysis at day 14. HEL and OVA were mixed together with alum (1:1 volume) and incubated shaking at 4 degree at least 1h before injection. Each mice received 100 μg of each antigens in 100 μL i.p. All experiments were approved by the local Animal Care and Use Committee.

Cells preparation for FACS and intracellular staining

Spleens were recovered immediately after euthanasia, perfused with complete cold medium, cut in small pieces and passed through a 70-μm filter. Cold ACK was used for red blood cell lysis and cells were then kept on ice in medium or complete medium depending on the experiments. For surface staining, cells were incubated for at least 30 mins on ice with antibodies. For intracellular labelling, cells were washed with cold PBS after surface staining and fixed for 20 min on ice with 2% PFA. Cells were washed once with BD Perm/Wash (554723) for WASp staining. Cells were resuspended in the respective permeabilization buffer containing 1:50 WASp-Alexa 647 from Santa Cruz clone B-9 and incubated at least 1 h on ice. Three washes with the respective permeabilization buffer were performed before FACS analysis.

RNA-seq

RNA-Seq was performed by the Genomic Technologies Facility of the University of Lausanne, Switzerland. Samples were obtained from sorted cells (DZ GCB: DAPI$^-$CD19$^+$GL7$^+$IgD$^-$CXCR4^{high}CD86^{low}) from control and GCBWcKO mice (n = 4). Total RNA was extracted using the RNeasy micro kit (Qiagen). Libraries were prepared as follow, RNA quality was assessed on a Fragment Analyzer (Agilent Technologies). The NEBNext Poly(A) mRNA Magnetic Isolation was used to isolate mRNA from 50 to 75 ng of total RNA. RNA-seq libraries were prepared using the NEBNext Ultra II Directional RNA Library Prep Kit for Illumina (New England Biolabs). Libraries were quantified by a fluorimetric method and their quality assessed on a Fragment Analyzer (Agilent Technologies).

Sequencing was obtained on an Illumina HiSeq2500 system. Purity-filtered reads were trimmed with Cutadapt for adapters and quality (v. 1.8). Reads matching to ribosomal RNA sequences were removed with fastq_screen (v. 0.11.1). Remaining reads were further filtered for low complexity with reaper (v. 15-065). Reads were aligned against Mus musculus.GRCm38.92 genome using STAR (v. 2.5.3a). The number of read counts per gene locus was summarized with htseq-count (v. 0.9.1). Quality of the RNA-seq data alignment was assessed using RSeQC (v. 2.3.7). Statistical analysis was performed using R (v. 3.5.1). Non-transcribed genes (i.e. with no counts across all samples) were filtered out. Cross sample normalisation was done using DESeq2 (v. 1.22.1). A batch effect was detected using principal component analysis (PCA) and clustering, it was thus removed using the RemoveBatchEffect function from Limma (v. 3.38.2). Differential gene expressions were obtained with the DESeq2 package. DESeq2 uses negative binomial GLM fitting and Wald-statistics. It operates on raw count data and internally normalizes the data. Default settings were used for estimating size factors for the normalization between samples and for estimating dispersions. The comparison CTL *vs*. GCBWcKO was performed and results for each comparison were obtained including p value adjustment by the Benjamini-Hochberg method for controlling for false discovery rate (FDR). Cooks cut-off and independent filtering were turned off. Differential expression was determined using an FDR <0.05. The 233 resulting genes were either manually characterized and clustered into functional groups based on the literature or subject to GSEA analysis.

TMRE, 2-NBDG and BODIPY-FL-C12 labeling

At 14 days p.i., 5 × 10^6 splenocytes/ml were incubated at 37°C for 30 min in RPMI, 10% FCS, 1% penicillin/streptomycin, 1% HEPES, 1% sodium pyruvate, 1% non essential amino acids supplemented with 200 nM TMRE or RPMI, 1% FCS supplemented with 100 nM BODIPY-FL-C12 or HBSS supplemented with 200 μM 2-NBDG. Cells (2 × 10^6) were then recovered, washed, and incubated on ice for surface staining.

CHIP array

Diluted sera (1:100) were loaded into a Tecan's HS 4800 Pro Hybridization Station. After hybridization, self-antibodies were revealed with Alexa Fluor 647 conjugated goat anti-mouse IgG Fab fragment specific (Southern Biotech 1015-31) at 10 μg/mL. Scanning and data alignment were performed with GenePix from Molecular Devices & ImaGene Software and Analysis with Qlucore.

ELISA

ssDNA or dsDNA from were added (2 μg/mL) to the Reacti-Bind DNA coating solution and in PBS for Ovalbumin (OVA) and Hen Egg Lyzozyme (HEL) (5 μg/mL). 50μL of antigens were added into Nunc immune plates and coated overnight at 4°C. Plates were blocked with PBS 1% BSA and then incubated with serial dilutions of serum for 1h. After washing, IgG-specific antibodies were detected by addition of anti-mouse IgG-HRP antibodies at 1:3000 for 1 h followed by TMB substrate (BD). The reaction was stopped with 2N sulfuric acid. Optical density (OD) was read at 450 nm.

J_H4 intron sequence mutation analysis

Bone marrow plasma cells (≥5,000 cells) were sorted as living B220$^-$IgD$^-$CD138$^+$ YFP$^+$ or YFP$^-$. Dry pellets were made and kept at −80°C until use. Pellets were resuspended in 10 μL of water and incubated 10 min at 95°C. After cooling, proteinase K was added for 30 min at 56°C for genomic DNA extraction. Amplification and sequencing of the J_H4 intronic region were performed using the primers and methods previously described (Le Gallou et al., 2018).

Cell cycle analysis

At 14 days p.i., 1 mg of EdU was injected i.p. in each mouse. Mice were sacrificed 1.5 or 6 h post-injection for analysis. Spleen were processed and splenocytes were surface labeled followed by EdU detection with Click-It Plus EdU Alexa Fluor 647 kit according to

the manufacturer's instructions. DAPI was then added to each sample (1 μg/mL). Samples were recorded at a very low speed (200 events/second) using a BD LSR II flow cytometer.

Histological analysis

Kidneys from 6-month-old mice were fixed in 4% formalin, paraffin-embedded and sectioned for PAS staining following standard techniques. A trained nephrologist assessed pathological damage blindly. Immunohistochemistry analysis of glomerular deposits of IgG was performed on frozen tissue sections using a goat anti-mouse IgG Alexa 488.

QUANTIFICATION AND STATISTICAL ANALYSIS

Statistics Statistical analysis was performed using GraphPad Prism software. The statistical significance of differences in mean values between two groups was analyzed by a two-tailed unpaired Student's t test with Welch's correction. Paired t test was performed only when comparing responses within the same experimental animal or tissue. In bar graphs for all figures, bars represent data mean. Error bars represent SD. ***$p \leq 0.001$; **$p \leq 0.01$; *$p \leq 0.05$; not significant, n.s. In all figures, unless otherwise noted, data points represent independent spleens.